# Characterization of some bioactive glasses based on$SiO_2$–CaO–$P_2O_5$–SrO quaternary system prepared by sol–gel method

K.M. Ereiba[1], A.S. Abd Raboh[1]* and A.G. Mostafa[2]

[1.]Biophysics branch, Faculty of Science, Al-Azhar University, Nasr City 11884, Cairo, Egypt.
[2.]Physics Department, Faculty of Science, Al-Azhar University, Nasr City 11884, Cairo, Egypt.
*ahmed1118343@yahoo.com

**Abstract:** Different bioactive glass samples of the composition [65%$SiO_2$–10%$P_2O_5$–(25-X)%CaO–X%SrO], Ca was gradually substituted by Sr (percentages of X= 0, 2, 4, 6, 8 and 10) have been prepared by sol-gel method. These samples were investigated from the structural point of view and the bioactivity by using different techniques: Evaluation of the crystallinity, crystal size, & the developed phases have been done using XRD technique, Assignment of the functional groups of the prepared samples by FTIR technique, Morphological observation of the resultant glasses was performed by (SEM). Dissolution of Ca and P were monitored periodically in physiological fluid which simulate the body fluid (SBF) by UV-Vis Spectrophotometer technique and biochemical Kits. The results showed that the substitution of Sr for Ca in the glass did not inhibit formation of calcium phosphate layer but retarded its precipitation rate, strongly dependent on Sr concentration. Crystal size and crystallinity of apatite peaks decreased gradually by addition strontium amount.
[Ereiba K.M, Abd Raboh A.S and Mostafa A.G. **Characterization of some bioactive glasses based on $SiO_2$–CaO–$P_2O_5$–SrO quaternary system prepared by sol–gel method.** *Nat Sci*2014;12(5):97-105]. (ISSN: 1545-0740).http://www.sciencepub.net/nature.13

**Keywords:** Bioactive glass; sol–gel; strontium; apatite

## 1. Introduction

Strontium, a trace element originally detected in lead mines near Strontian (Scotland) in the late 1700s, It is found in the mineral compounds Celestine ($SrSO_4$) and Strontianite ($SrCO_3$), which are present in soil and drinking water. [1, 2]

Pioneer experiments on animals showed that strontium salts can decrease bone resorption and increase bone formation and bone mass without affecting bone mineralization, raising the possibility that strontium may be of potential benefit for treatment of osteoporosis. [3–6]

Beside its chemical analogy to Ca, Sr is a bone seeking element and 98% of the total body Sr content can be found in the skeleton. After administration of Sr salt, it passes through the Haversian capillaries walls by diffusion to reach the bone extracellular fluid and finally deposit in the bone, being adsorbed on the bone apatite surface or substitute Ca in bone crystals. $Sr^{+2}$, having ionic radius (1.13 Å) higher than that of $Ca^{+2}$ (0.99 Å), its incorporation in bone crystals increases the length of Sr-hydroxyl bond more than that of Ca-hydroxyl. This in turn results in a decrease in the lattice energy, which is inversely proportional to the cohesion distance and, therefore, a subsequent decrease in crystallinity. Thus, Sr incorporation in bone mineral may lead to the modifications in lattice parameters, crystal size, and crystallinity of bone mineral. [7, 8]

The SrO/CaO substitution becomes a new strategy in designing new bioactive materials as strontium and calcium are similar in chemical nature and the substitution will not considerably change the basic chemical and physical properties of calcium containing bioactive glass and ceramics, such as Bioglasses, hydroxy apatite, and calcium phosphates. Thus the SrO/CaO substitution can lead to a new strategy for creating materials for bone repair and regeneration therapy. Together with the effect of surface bioactivity of bioactive glasses, gene activation effect of their ionic solutions, and the promotion of bone growth due to strontium ion release, it is possible to create new bioactive materials based on existing bioglass compositions with Sr/Ca substitution to combine bone bonding and osteoblast stimulating effects. These glasses can be used as an effective material for bone regeneration that can find applications in dental, implants, and other biomedical applications. Strontium containing glasses can also be used as a strontium ions delivery media by controlled dissolution in body fluid environment. There is very limited structural information of strontium containing glasses, especially in those close to the bioglass composition. Except the atomic structure of strontium substituted glasses, understanding the dynamics and dissolution behavior of strontium containing bioactive glasses can play a key role in developing these glasses for various biomedical applications. [9]

The present study investigates the effect of strontium substitution for calcium on bioactivity of sol–gel derived Sr-containing glasses. Prepare six

different bioactive glass samples composed of $65SiO_2$–(25-x)-CaO–$10P_2O_5$–(x)SrO)], Ca was gradually substituted with Sr (percentages of *0, 2, 4, 6,8 and10*) by sol-gel method. Investigate the structure and bioactivity of these samples by using different techniques: (DSC), (XRD), (FT-IR), (SEM) and (EDXA). Study the resorbability and dissolution of prepared samples in physiological fluid which simulate the body fluid SBF and perform some spectrophotometer analysis using biochemical Kits.

## 2. Materials and methods

### Preparation of samples

Glass composition was (65% $SiO_2$, 25% CaO, 10% $P_2O_5$, mol%) named Sr(0) was used as a control sample and CaO was gradually replaced by SrO ( percentages of 2, 4, 6, 8 and 10 mol%) in its composition. The sol–gel synthesis of the glass of composition $SiO_2$–$P_2O_5$–CaO–SrO was prepared using stoichiometric amount of precursors and the gels were obtained as the method described previously[10].Initially, tetraethoxysilane[Si $(OC_2H_5)_4$] (TEOS) was added to 0.1 M nitric acid and the mixture was allowed to react for 60 min for the acid hydrolysis of TEOS. Then a series of reagents was added in the following sequence, allowing 45 min for each reagent to react completely: triethylphosphate [PO $(OC_2H_5)_3$] (TEP), calcium nitrate tetra hydrate-[Ca $(NO_3)_2.4H_2O$] and strontium nitrate [Sr $(NO_3)_2$]. Tetraethoxysilane, triethylphosphate, calcium nitrate tetra hydrate, and strontium nitrate were purchased from Sigma-Aldrich. After the final addition, mixing was continued for 1 h to allow the completion of hydrolysis. The Sr-free bioglass sample was also synthesized by the same procedure to compare its bioactivity with that of the Sr-substituted bioglass. $NH_4OH$ (10ml) added to the resulted solution for gelation. The resultant gel was kept in a sealed container and heated at 70 ºC for an additional 3 days. The water was removed and a small hole was inserted in the lid to allow the leakage of gases while the gel was heated to 120 ºC for 2 days to remove all the free water. The dried gel was then heated for 24 h at 800 ºC to stabilize the glass and eliminate residual nitrates.

### Characterization techniques

The DSC/ TG characterization of the dried gel was conducted in Differential Scanning Calorimeter (DSC) [computerized SETARAM labsys™] Thermal Analyser. The sample was heated in flowing Argon gas atmosphere at a heating rate of 10ºC/min. The weight loss measurements were also done in the same instrument and both the graphs were merged into one for comparative analysis. Phase analysis of the samples was examined by X-ray diffractometer (XRD); model BRUKER axs, using Ni-filtered CuKα radiation at 40 kV, 25 mA and λ (1.54A°). FTIR absorption spectra were recorded at room temperature in the 400 – 4000 $cm^{-1}$ range using a spectrometer of type (FT-IR-400, JASCO, and Japan). The obtained spectra were used to analyze the structure of glasses before and after immersion in the simulated body fluid (SBF).

Morphological observation of the resultant glasses was performed by Philips XL 30 scanning electron microscope (SEM) with an accelerating voltage of 30 kV. Specimens were placed on a stub using a carbon sticker and examined under the microscope after being sputtered with a thin coat of gold. Elemental image analysis was also carried out using energy dispersive X-ray analysis ((EDXA; 30 $mm^2$ Si (Li) R-RSUTW detector)) coupled to the SEM instrument. EDX used to compare the intensities of calcium (Ca), phosphor (P) in bioglass before and after immersion in SBF. The changes in concentration of Ca, P of the extracted SBF solution were measured by UV-Vis Spectrophotometer technique.

### *In vitro* bioactivity analysis:

### Immersion in SBF

Hydroxy apatite forming ability of the bioglass disks was studied by immersing the samples in simulated body fluid (SBF) for different periods. Each specimen was immersed in tris-buffered SBF solution with ion concentrations and pH nearly equal to that of human blood plasma (Table 1) at 37 ± 0.5ºC, for 21 days. A surface area to volume ratio of 0.1 $cm^{-1}$ was maintained for all immersions, and the SBF solutions were not exchanged during the experiments.

The SBF was prepared by dissolving reagent-grade NaCl, $NaHCO_3$, KCl, $K_2HPO_4$ , $3H_2O$, $MgCl_2$ , $6H_2O$, $CaCl_2$, and $Na_2SO_4$ in deionized water. The solution was buffered to a pH of 7.4 with tris–(hydroxymethyl)-amino methane ($(CH_2OH)_3CNH_3$) and hydrochloric acid [11]. The samples were removed from the incubator, rinsed gently, first with pure ethanol and then using deionized water, and left to dry at ambient temperature in desiccators for 3 h.

Changes in phase structure of the specimens were determined by X-ray diffractometry (XRD). After 21 days of soaking in SBF, the samples were withdrawn from the solution and washed with distilled water, dried at room temperature, ground to fine powder and analyzed. XRD has been made for all samples with Co Kα (1.54A°) radiation, identified by JCPDS International Center for Diffraction Data Cards. The patterns of unsoaked bioactive glass specimens were also taken for comparison.

FTIR spectra of the bioactive glasses were measured at room temperature in the wave number range of 4000–400 $cm^{-1}$. Fine powders were mixed with KBr powder by the ratio of 1:100. The FTIR spectra were immediately measured after preparation of the disc. The obtained spectra were used to analyze the structure of glasses before and after immersion in (SBF).

Change in the concentration of Ca and P ions in the SBF was measured soaking the powder samples in 80 ml of SBF in polyethylene containers maintained at 37 ˚C for 21 days. During the course of immersion the dissolution of Ca and P ions into the SBF solution was monitored periodically using UV-Vis Spectrophotometer technique.

Table. Concentration (mM) and pH of (SBF) and human plasma. [12]

| Ion | SBF (mM concentration) | Plasma (mM concentration) |
|---|---|---|
| Na+ | 142 | 142 |
| K+ | 5.0 | 5.0 |
| Mg++ | 1.5 | 1.5 |
| Ca++ | 2.5 | 2.5 |
| $Cl^-$ | 147.8 | 103.0 |
| $HCO_3^-$ | 4.2 | 4.2 |
| $HPO_4^{--}$ | 1.0 | 1.0 |
| $SO_4^{2-}$ | 0.5 | 0.5 |
| pH | 7.25 | 7.20-7.40 |

## 3. Results and discussion

### DSC and TGA thermal analysis

The obtained DSC, TG curves of Sr (4%) powder, heated up to 1000˚C are shown in Fig (1).The total weight loss shown in TG curve is about 36wt%.The first weight loss occurred in the temperature range of 25–180 ˚C (less 3.10 wt%) can be ascribed to the loss of alcohol and water. The second weight loss (13.70 wt %) occurred in the range of 180–320˚C is associated with the partial elimination of organic residues which is confirmed by the corresponding endothermic signal in the DSC curve. Very slow heating in this temperature range was very important to eliminate the remaining organics. More weight loss commenced from the end of first weight loss (280˚C) up to 600˚C, which is most likely due to the loss of organic moieties by further condensation. The maximum weight loss rate takes place between 300 and 500˚C, thus the gels were further calcined at 500˚C to remove organic residuals; the weight loss above that temperature may due to the elimination of hydroxyls. In general, the dried gels showed overall weight losses around 20–30% over the temperature range 50–800˚C during the course of TGA measurements.

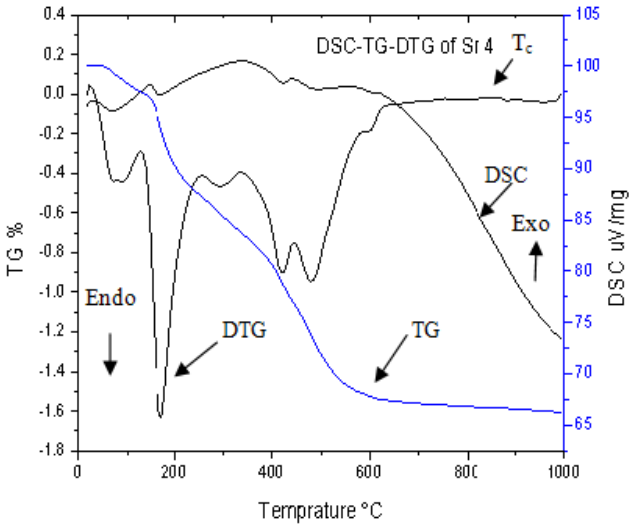


Figure 1. The DSC–TG curves of Strontium (4%) containing glass.

DSC trace is a plot of heat changes of the glass as a function of temperature and is used to determine temperatures at which phase transitions or another thermal phenomenon occur. The first endothermic peak observed in the range of 158–194˚C is attributed to the loss of the residual solvent (water and ethanol).The second endothermic peak (onset at 451˚C) was due to the condensation of silanol groups and the removal of nitrate groups that are usually eliminated in the thermal stabilization process. All nitrates were removed at 550˚C.Also,the small exothermic peak corresponded to crystallization of the glasses is appeared at 890 ˚C for BG-Sr .Theoretical density of SrO is 4.7 $g/cm^3$ that is much higher than that of CaO, i.e. 3.4 $g/cm^3$. This leads to increase in powder density of the glass specimen when Ca is replaced by Sr in its composition. The increase in density also correlates with an increase in the Tg and couples with a shift in crystallization temperature. Glass transition refers to transformation from glassy state (rigid form) into glass forming liquid during heating. Glass transition depends on the movement of the glass building units. Glasses with higher Tg require more energy to rearrange covalent bands in the amorphous lattice.

It is suggested that the required energy for breaking Sr–O bond in Si–O–Sr group is higher than that of Ca–O in Si–O–Ca group due to higher electro negativity of Sr in comparison with Ca.[13]

**X-Ray diffraction**

Fig (2) shows the XRD pattern of the glass samples containing various amounts of Sr before immersion in SBF. All samples were devoid of crystalline peaks and take amorphous state characterized by the broad diffraction bands centered approximately at 2θ = 25 in, indicate the internal disorder and glassy nature of these materials.

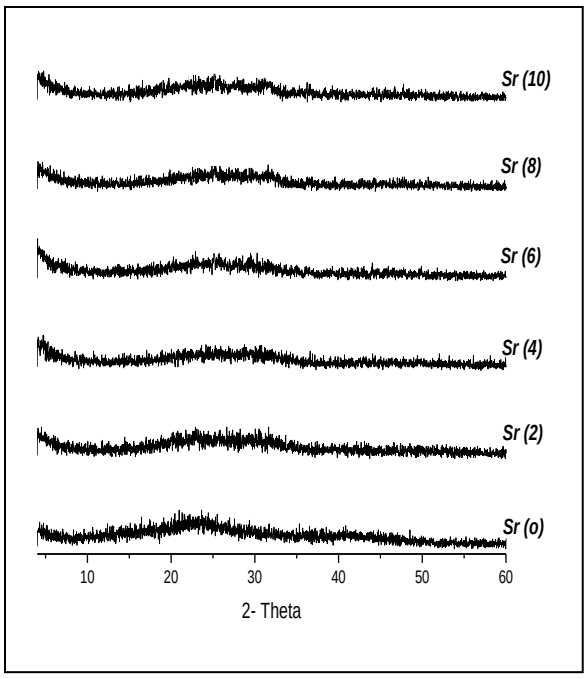


Figure 2. XRD pattern of the glass samples containing various amounts of Sr before immersion in SBF.

Fig (3) shows the XRD pattern of the glass samples containing various amounts of Sr after immersion in (SBF) for 21 day, where some crystalline peaks appear in the XRD patterns, indicating the formation of a crystalline layer on the surface of the glass. Initially, two well-defined hydroxy apatite (HA) peaks develop at 2θ values of 2θ=31.8° (211) and 25.8° (002) according to the standard JCPDS cards (76-0694). Wide diffraction peak at angles (2θ) at 32.18°, 32.8° corresponds to the overlapping of (1 1 2), (3 0 0) reflections planes of the well- crystallized HA. Characteristic peaks of apatite were observed in the patterns of all specimens with higher peak intensity for control sample Sr (0) and samples that contained lower amounts of Sr (Sr (2), Sr (4) and Sr (6)), but intensity of apatite peaks decreased in Sr (8) and Sr (10).From the XRD patterns it was found that the rate of in vitro apatite formation on bioactive glasses decreased with increasing the amount of Sr in the glass composition. These results confirmed the previous studies. [14]

**Calcite ($CaCO_3$) peaks**

It is notable that in Sr (0) Sr (2) and Sr (4) there are two well-defined calcite ($CaCO_3$) peaks develop at 2θ values 29°and 48° according to the standard JCPDS cards (88-1809). Calcite peaks disappeared in other samples that contained higher amounts of strontium.

**Strontianite ($Sr CO_3$) peaks**

Also, three major peaks located at around 25.18°, 25.83° and 44.7° can be attributed respectively to (111), (021) and (041) reflection plans of the ($SrCO_3$) according to the standard JCPDS cards (84-1778). Strontianite ($SrCO_3$) peaks became sharper as the Sr concentration increased. [14]

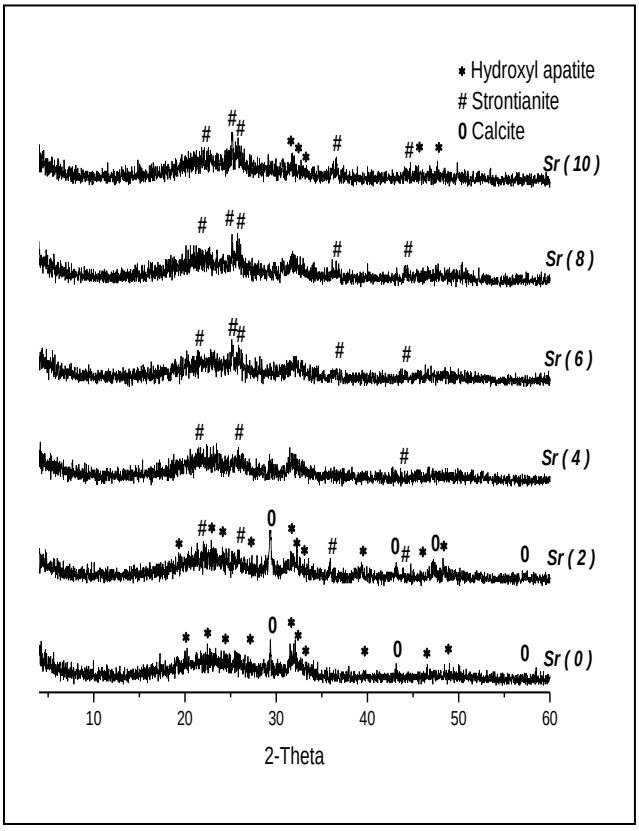


Figure 3. XRD pattern of the glass samples containing various amounts of Sr after immersion in SBF.

**Evaluation of crystallinity**

Degree of crystallinity (**$X_C$**), corresponding to the fraction of crystalline phase present in the examined sample, was evaluated by the relation: [15], [16]

$$X_c = 1 - \frac{V_{112/300}}{I_{300}}$$

Where I is the intensity of the main peak reflection, V is the intensity of the hollow between the main peak and the first neighbor peak.

**Determination of crystallites size by Scherer's equation**

The crystallite size (**L**) was calculated from the broadening in the XRD pattern. According to Scherer's equation L is given by: [16]

$$L = \frac{K\lambda}{\beta\ Cos\theta}$$

Where (**β**) is the full width of the peak at half of maximum intensity (FWHM) (in radians), (**λ**) is the wavelength of the used X-ray beam (λ=1.54 Å) , ($\theta$) is the diffraction angle, (**K**) is a Scherer constant defined as the crystallite shape and is approximately equal 0.9.It was found that the crystal size and crystallinity of apatite peaks (211) and (002) decreased gradually by increasing strontium content Fig (4).

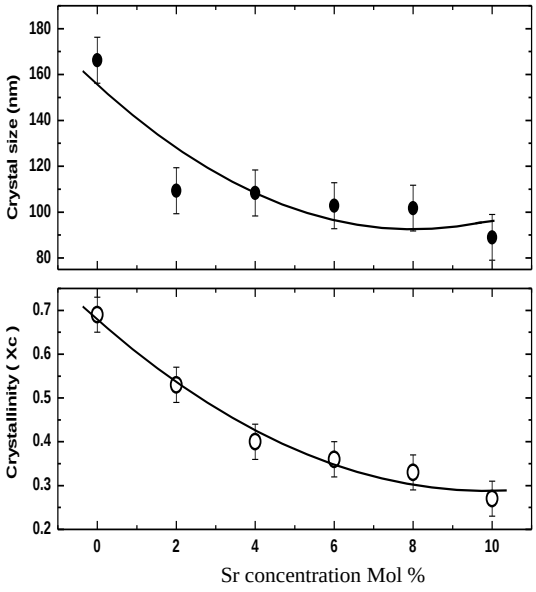


Figure 4. Crystal size and crystallinity of apatite peaks (211) and (002).

The broad peaks observed at 2θ=31.8 and 25.8° reflect presence of (211) and (002) atomic planes with poor crystallinity in apatite lattice, The diffraction peaks of apatite layer 2θ=31.8° (211) shifted to lower 2θ values with Sr-addition, indicating an increase in d-spacing and hence lattice parameters. This would be expected as Sr is slightly larger than Ca (118 and 100 pm for octahedral coordination.

The replacement may cause a significant increase in glass solubility due to increasing the network disorder caused by higher ionic radius of Sr compared with Ca as well as increasing in surface area. The increased disorder can cause an increase in glass solubility, because solubility is a trade-off between the energy required to dissociate the structure and the energy released upon hydration of the resultant ions. Therefore, it seems reasonable to suggest that a more disordered network produces a less stable (or more soluble) structure. Sr cations can also block sites of calcium phosphate nucleation. Note that Sr did not inhibit formation of calcium phosphate layer but retarded its precipitation rate. Generally it have been suggested that CP crystallization was restricted on the surfaces of the Sr-containing bioactive glasses, especially in specimens with high dose of Sr. This is in agreement with our study, Sr seems that retards formation of CP in any visible way. [13, 14]

**Fourier transforms infrared spectrometer (FTIR)**
**Before immersion**

For all unsoaked glasses Fig (5), shows the bands appeared in the range 800–1100 $cm^{-1}$ are ascribed to the stretching modes of $SiO_4$ tetrahedra. The wide absorption band at 1000–1100 $cm^{-1}$ assigned to the asymmetric stretching mode Si–O (asym), the weak band around 800 $cm^{-1}$ is associated to symmetric stretching vibration Si–O–Si (sym). Furthermore, the band at 470 $cm^{-1}$ can be ascribed to the Si–O–Si bending mode. The signals at around 1630, 3433 $cm^{-1}$ is also assigned to deformation mode of H–O–H group attributed to the absorbed water molecules.

In Sr (0), the band observed at 460 $cm^{-1}$ is attributed to bending mode of Si–O–Si that shifted to wave number of 470 $cm^{-1}$ in spectra of Sr-containing samples. The bands corresponding to bending mode of Si–O–Si group observed in 1215 $cm^{-1}$ in the spectrum of Sr (0) also shifted to 1225 $cm^{-1}$ in Sr-containing glass. The bands appeared around 560 are corresponded to P–O bending vibrations.

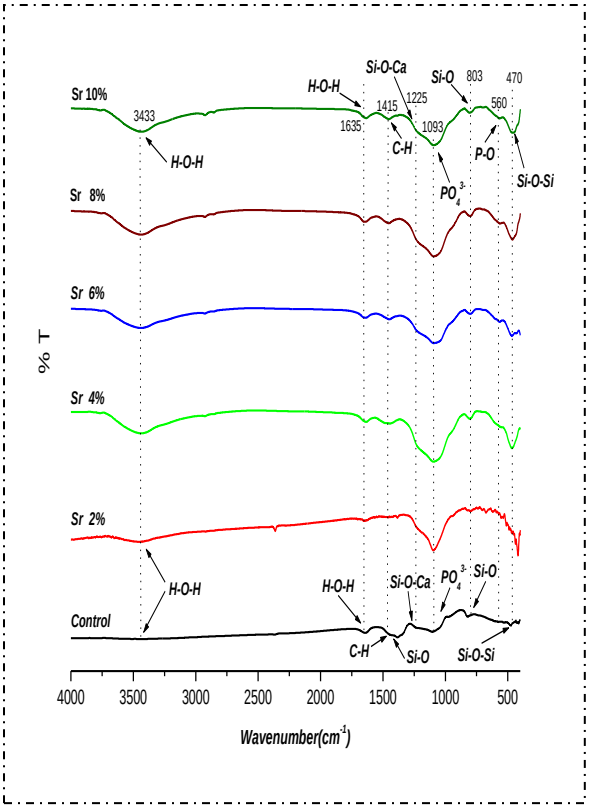


Figure 5. The obtained FT-IR transmittance spectra for Sr containing glass before soaking in SBF solution.

**After immersion**

The sharpened bands in the range of 800 – 1100 $cm^{-1}$ are probably due to the formation of silica gel like layer on the surfaces of these glasses Fig (6).

The peaks at 570 $cm^{-1}$ are associated with the P–O bending mode of crystalline phosphate (apatite) formed on the glasses and the shoulder appeared at 870 $cm^{-1}$ is attributed to the stretching (str) mode of C–O group in the lattice structure of the formed apatite layer. The absorption band at around 1050 $cm^{-1}$ associated with the P–O stretching has an overlap with Si–O–Si (asy) and thus is not clearly distinguishable. The shoulder that appeared in all samples at 1246 $cm^{-1}$ is related to the non bridging oxygen bonds (NBO) of Si–O–Ca. Two bands located at 1620 and 3423 $cm^{-1}$. These absorption bonds are characteristic of the presence of water related to the hygroscopic feature of the formed apatite. The bands that appeared at 875 and 1422 $cm^{-1}$ are assigned to C–O stretching in carbonate groups substituted for phosphate groups in apatite lattice.

It is notable that the SrO may be able to enter the forming apatite nuclei and thus inhibits their evolution to tiny apatite crystals. This can be considered for SrO cannot be accommodated in the apatite structure (the apatite lattice) but changes in its physicochemical properties. [17]

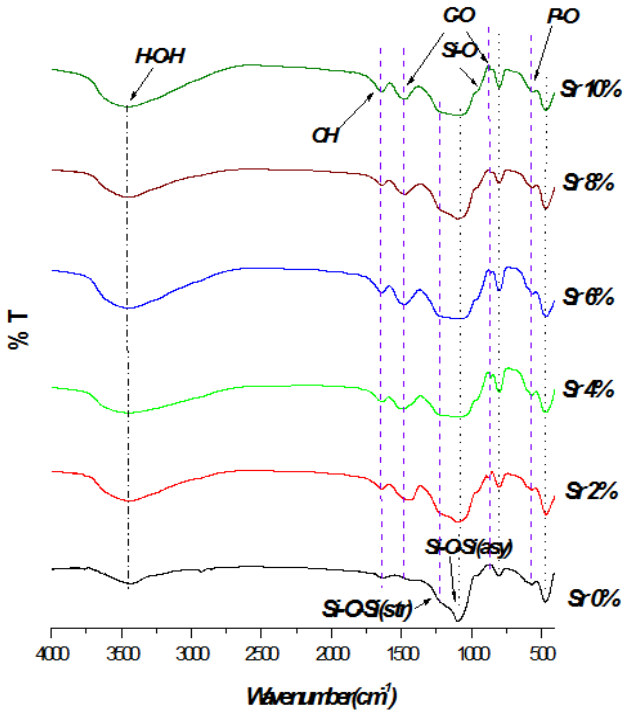


Figure 6. The obtained FT-IR transmittance spectra for Sr containing glass after soaking in SBF solution.

**Surface morphology and elemental composition**

Fig (7) shows SEM image-EDXS spectrum of the 4% Sr-bioglass sample before indicating the nominal composition of strontium substituted bioglass.SEM of the glass surface revealed a heterogeneous surface. EDXS spectrum shows the presence of Si , P, Sr and Ca as the main elements in the network.

Fig (8) shows SEM micrographs of the 4% Sr-bioglass soaked in SBF for 21 days. Flake-like crystals with different abundance are observed on glass matrix. The flakes seems that covered limited amount of these crystals are formed on the surfaces of 4% Sr-bioglass sample. These flake-like crystals have been expressed that are precipitated calcium phosphate with bone-like morphology. This is in agreement with previous studies. [18]

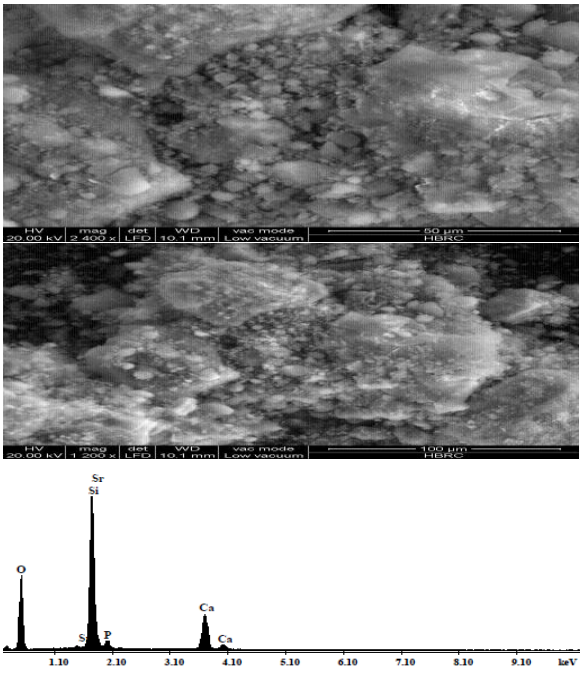


Figure 7. SEM image -EDXS spectrum of (4% Sr-bioglass) before immersion indicating the nominal composition and the heterogeneity nature of Sr substituted bioglass.

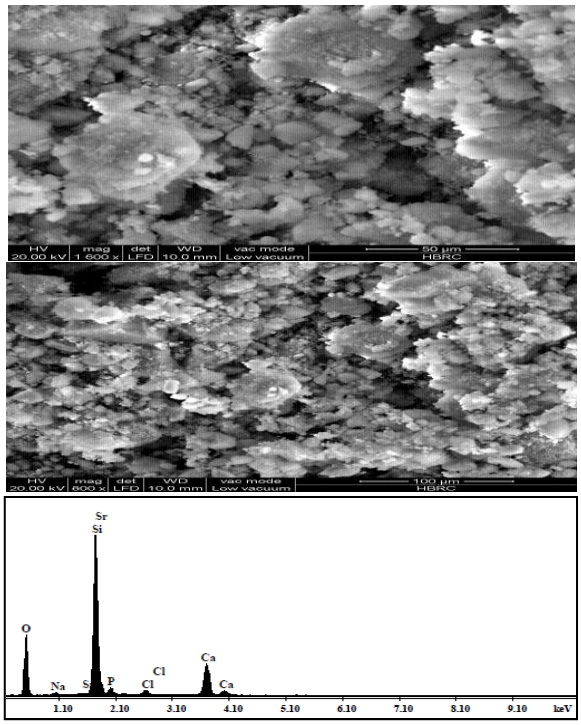


Figure 8. SEM image – EDXS microanalysis of 4% Sr-bioglass surface after 21 days of immersion in SBF.

The elemental image analyses of Sr 4% sample carried out by EDXS, Fig (8) shows the presence of P and Ca as the main elements of glass surface and confirm that the formed layers are calcium phosphatic in nature. The presence of Si peak with reduced intensity is also noticeable. It originates from the underneath layer of the (glass) and its reduced peak intensity reveals considerable thickness of the formed layer. The peak corresponded to Cl suggests that this ion is incorporated into the crystal structure of apatite or adsorbed on glass surfaces from the SBF despite of washing process. [13, 17, 18]

**Elemental analysis**

**Calcium concentration**

Fig (9) shows the absolute concentration of Ca, P ions in SBF solution. The change in concentration of Ca ions can reflect the competition condition between the rate of dissolution and precipitation processes. At t=0, concentration of calcium in SBF solution is approximately 100 mg/L. The increase in Ca concentration observed for all specimens at the end of the first day is attributed to dissolution of the bioglass phase. The rate of dissolution decreased in day 2 up to 21 day in Sr (0) and Sr-containing samples.

The Ca concentration was found to be higher than 100 mg/L which means that the dissolution rate is faster than the precipitation rate and it is the opposite for the Ca concentrations which is lesser than 100 mg/L.

It is found from the results that the precipitation of calcium phosphate onto the surfaces of the bioglasses is postponed by incorporation of Sr ions into the glass matrix. Furthermore, substitution of Ca with Sr ions in the glass composition increased the solubility of the bioactive glass, because Ca concentration of those SBF that contained Sr-bioglass specimen was higher than that of Sr (0). Decreasing in the $Ca^{2+}$ concentration in SBF is attributed to the rapid growth of the apatite nuclei formed on the surface of the glass that overcame the release rate of calcium ions to the solution. The pH varied corresponding to $Ca^{2+}$ concentration variations, because $Ca^{2+}$ in the glass exchanged with $H^+$ or $H_3O^+$ in the SBF. This means that a layer of apatite formed in all sample, but the surface area decreased by increasing Sr concentration. So free surface area on the glass samples increased by increasing strontium oxide. This may be due to more concentration of Ca dissolved from the glass surface as the free surface increased. [19]

**Phosphorus concentration**

Fig (9) shows the concentration of P ions in SBF solution after 21 days of immersion. Before immersion phosphate ion concentration in SBF is 30% only. After immersion of samples in SBF for 21 day, at 24 h it is noted that phosphate concentration in all glass samples increased to high values due to the release of phosphate from these samples to the solution but decreased gradually after 24h to reach low values indicating the consumption of phosphate in the formation a layer of crystalline HCA on the surface of glass.

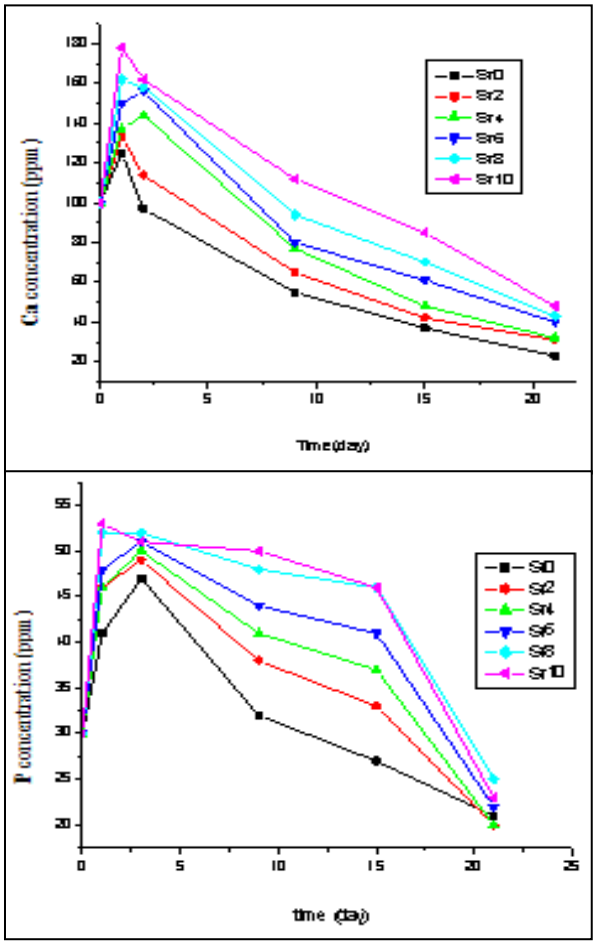


Figure 9. The concentration of **Ca** (upper), **P** (lower) ions in SBF solution versus time.

**pH analysis**

The pH increased during the first 24 h of the process as a consequence of partial dissolution that gives an idea of the high reactivity of these materials. These facts agree with the formation mechanisms of the apatite layer on bioactive glass and glass ceramics, *i.e.*, in early stages, an interchange takes place between $Ca^{2+}$ and $H_3O^+$ ions from the solution. Such interchanges provoke an increase in pH that favors the formation of apatite nuclei on the silanol groups in the glass surface.

The formation of apatite in SBF is strongly pH dependent; the increase in pH actually signifies for the reduction in the concentration of $H^+$ due to the replacement of metal ions in the glass and subsequent production of $OH^-$ groups due to breaking of siloxane bond. [20] The variation of pH values relative to soaking times in SBF of all samples are shown in Fig (10). After 48 hour pH increased until reach a value of 8.07 Sr (0), 8.211 (Sr (2), 8.251 (Sr (4), 8.249 (Sr (6), 8.261 (Sr (8), 8.312 (Sr (10). From the third day up to 15 day, the pH decreased gradually until reach 7.625 Sr (0), 7.829 (Sr (2), 7.836 Sr (4), 7.875 Sr (6), 7.881Sr (8), 7.945 Sr (10).

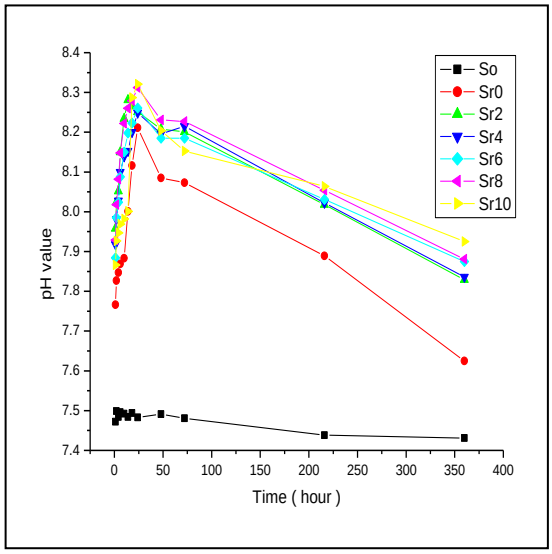


Figure 10.The change in pH results of Sr (0) to Sr (10), compared by reference sample $S_0$ , after immersion in SBF solution for 15days.

The fluctuation in pH value of all samples may be explained when considering the result of two opposite processes: the release of $Ca^{2+}$ from the glass, and the consumption of $Ca^{2+}$ due to the formation of apatite layer. Therefore, when the releasing rate of $Ca^{2+}$ is higher than the consumption rate, the pH will increase, or else, the pH will decrease. It is found from the results that substitution of Ca with Sr ions in the glass composition increase the solubility of the bioactive glass, which subsequently increase the interchange $Ca^{2+}$ and $H_3O^+$ ions from the solution and increase the pH value.

**Conclusion**

Different bioactive glass samples were prepared having the composed of [$SiO_2$-CaO–$P_2O_5$–SrO)], Ca was gradually substituted with Sr (0, 2, 4, 6, 8 and

10) by sol-gel method. The results showed that substitution of Ca with Sr ions in the glass matrix increased the solubility of the bioactive glass and did not inhibit the formation of calcium phosphate layer, but retarded its precipitation rate. SEM micrographs of the 4% Sr-bioglass soaked in SBF for 21 days showed Flake-like crystals with different abundance are observed in the glass matrix. The flakes seem to cover limited amount of these crystals are formed on the surfaces of 4% Sr-bioglass sample, strongly dependent on Sr concentration. Crystal size and crystallinity of apatite peaks decreased gradually by addition strontium amount.

**Correspondence to:**
Ahmed. S. Abd Raboh
Biophysics branch, Faculty of Science
Al-Azhar University, Nasr City 11884, Cairo, Egypt.
Emails: ahmed1118343@yahoo.com

**Reference**

1. Marie P, Neve J, Chappuis P, Lamand M. Effects of strontium on bone formation and bone cells, In Therapeutic Uses of Traces Elements. New York Plenum Press1996; 277-282.
2. Nielsen S. The biological role of strontium. Bone2004; 35:583-588.
3. Marie P, Garba T, Hott M, Miravet L. Effect of low doses of stable strontium on bone metabolism in rats. Miner Electrolyte Metab1985; 11:5-13.
4. Marie P, Hott M. Short-term effects of fluoride and strontium on bone formation and resorption in the mouse. Metabolism 1986;35: 547-551.
5. Grynpas M, Marie P. Effects of low doses of strontium on bone quality and quantity in rats. Bone 1990; 11: 313-319.
6. Grynpas M, Hamilton E, Cheung R, Tsouderos Y, Deloffre P, Hott M, Marie PJ. Strontium increases vertebral bone volume in rats at a low dose that does not induce detectable mineralization defect. Bone1996; 18:253-259.
7. Kendler L. Strontium ranelate—data on vertebral and non vertebral fracture efficacy and safety: mechanism of action. Curr Osteoporosis Rep 2006; 4: 34-9.
8. Boivin G, Deloffre P, Perrat B.Strontium distribution and interactions with bone mineral in monkey iliac bone after strontium salt (S 12911) administration. J Bone Miner Res 1996; 11: 1302-11.
9. Jincheng D, Xiang Ye. Effect of strontium substitution on the structure, ionic diffusion and dynamic properties of 45S5 bioactive glasses. Journal of Non-Crystalline Solids 2012; 358:1059–1071.
10. El-Gohary M, Tohamy K, El-Okr, Islam E. Soliman. Influence of composition on the in-vitro bioactivity of bioglass prepared by a quick alkali-mediated sol–gel method. Nature and Science 2013; 11(3):26-33.
11. Kokubo T, Kushitani H, Sakka S, Kitsugi T, Yamamuro T. Solutions able to reproduce invivo surface-structure changes in bioactiveglass–ceramic A-W. Biomed Mater Res 1990; 24:721–34.
12. Fujibayashi S, Neo M, Kim H-M, Kokubo T, Nakamura T. A comparative study between in vivo bone ingrowths and in vitro apatite formation on $Na_2O–CaO–SiO_2$ glasses. Biomaterials 2003; 24:1349–1356.
13. Hesaraki S., Mozhdeh G., Sadaf V., Sara S. The effect of Sr concentration on bioactivity and biocompatibility of sol–gel derived glasses based on $CaO–SrO–SiO_2–P_2O_5$ quaternary system. Materials Science and Engineering.2010;30 :383–390.
14. Taherkhania S, Fathollah M. Sol-gel synthesis and characterization of unexpected rod-like crystal fibers based on $SiO_2$-(1-x) CaO-xSrO-$P_2O_5$ dried. Non-Crystalline Solids 2012; 358:342 – 348.
15. Heijligers H, Driessens F, Verbeeck R. Lattice-parameters and cation distribution of solid-solutions of calcium and strontium hydroxyapatite. Calcified Tissue Int 1979; 29(2): 127–31.
16. Cullity D. Elements of X-ray diffraction. Reading, MA: Addison- Wesley; 1959.
17. Shahrabi S, Hesaraki S, Saeed M, Mina K. Structural discrepancies and in vitro nanoapatite formation ability of sol–gel derived glasses doped with different bone stimulator ions. Ceramics International2011; 37: 2737–2746.
18. Wafa I, El-Sayed M. Comparative study of $Sr^{+2}$ and $Zn^{+2}$incorporation in the biomimetic coating of a prosthetic alloy. The Open Biomaterials2011; 3: 4-13.
19. Peitl O, Zanotto D, Hench LL. Highly bioactive $P_2O_5–Na_2O–CaO–SiO_2$glass–ceramics. Non-Cryst Solids2001; 292:115–126.
20. Zhang Y, Santos J. Micro structural characterization and in vitro apatite formation in $CaO–P_2O_5–TiO_2–MgO–Na_2O$ glass–ceramics. J. Eur. Ceram. Soc 2001; 21: 169–175.